https://doi.org/10.1093/plcell/koac008 THE PLANT CELL 2022: 34: 1273–1288

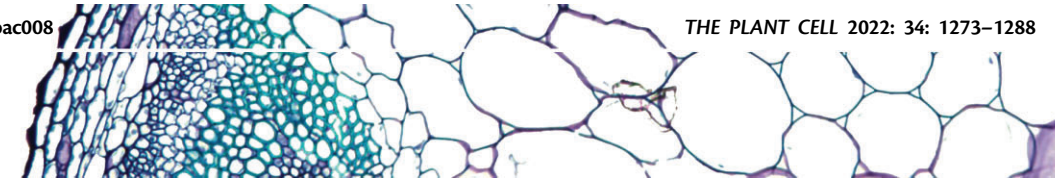

Research Article

Orchestration of ethylene and gibberellin signals determines primary root elongation in rice

Hua Qin [1,5,†] Bipin K. Pandey [2,†] Yuxiang Li [1,†] Guoqiang Huang [3,†] Juan Wang [1,5] Ruidang Quan [1,5] Jiahao Zhou [1] Yun Zhou [4] Yuchen Miao [4] Dabing Zhang [3,*] Malcolm J. Bennett [2,*] and Rongfeng Huang [1,5,*,‡]

1 Biotechnology Research Institute, Chinese Academy of Agricultural Sciences, Beijing 100081, China
2 Future Food Beacon and School of Biosciences, University of Nottingham, Nottingham LE12 5RD, UK
3 School of Life Sciences and Biotechnology, Shanghai Jiao Tong University, Shanghai 200240, China
4 Collaborative Innovation Center of Crop Stress Biology, Institute of Plant Stress Biology, Henan University, Kaifeng 475001, China
5 National Key Facility of Crop Gene Resources and Genetic Improvement, Beijing 100081, China

*Author for correspondence: rfhuang@caas.cn (R.H.), malcolm.bennett@nottingham.ac.uk (M.J.B.), and zhangdb@sjtu.edu.cn (D.Z.)
†These authors contributed equally to this work.
‡Senior author.

R.H., M.J.B., D.Z., H.Q., B.K.P., and G.H. conceived the project and analyzed the data. H.Q., B.K.P., Y.L., J.W., R.Q., and J.Z. performed the experiments. Y.Z. and Y.M. provided useful suggestions. D.Z., M.J.B., H.Q., and R.H. wrote the manuscript.
The author responsible for distribution of materials integral to the findings presented in this article in accordance with the policy described in the Instructions for Authors (https://academic.oup.com/plcell) is: Rongfeng Huang (rfhuang@caas.cn).

Abstract

Primary root growth in cereal crops is fundamental for early establishment of the seedling and grain yield. In young rice (*Oryza sativa*) seedlings, the primary root grows rapidly for 7–10 days after germination and then stops; however, the underlying mechanism determining primary root growth is unclear. Here, we report that the interplay of ethylene and gibberellin (GA) controls the orchestrated development of the primary root in young rice seedlings. Our analyses advance the knowledge that primary root growth is maintained by higher ethylene production, which lowers bioactive GA contents. Further investigations unraveled that ethylene signaling transcription factor ETHYLENE INSENSITIVE3-LIKE 1 (OsEIL1) activates the expression of the GA metabolism genes *GIBBERELLIN 2-OXIDASE 1* (*OsGA2ox1*), *OsGA2ox2*, *OsGA2ox3*, and *OsGA2ox5*, thereby deactivating GA activity, inhibiting cell proliferation in the root meristem, and ultimately gradually inhibiting primary root growth. Mutation in *OsGA2ox3* weakened ethylene-induced GA inactivation and reduced the ethylene sensitivity of the root. Genetic analysis revealed that OsGA2ox3 functions downstream of OsEIL1. Taken together, we identify a molecular pathway impacted by ethylene during primary root elongation in rice and provide insight into the coordination of ethylene and GA signals during root development and seedling establishment.

Introduction

Plant roots mediate water and nutrient uptake from the soil and provide mechanical support for shoot growth (de Dorlodot et al., 2007; Shekhar et al., 2019). Thus, a healthy root system is essential for a healthy plant; as the Chinese proverb goes, deep and developed roots make flourishing leaves. The root systems of dicots consist of a primary root and lateral roots; the continuous growth of the primary root is required for plants to complete their lifecycles (Tian et al., 2014; Zheng et al., 2016). Unlike dicots, the primary root of monocots such as rice (*Oryza sativa*) exhibits determinate

Received August 16, 2021. Accepted January 06, 2022. Advance access publication January 11, 2022

IN A NUTSHELL

Background: The optimization of root architecture is one of the most effective ways to improve crop productivity and stress resistance. The primary root, which emerges when the seed germinates, is critical for plant establishment and survival, providing the seedling with its sole source of anchorage and water/nutrient absorption. In rice, the primary root ceases to grow after 7–10 days of rapid growth; however, the underlying mechanism determining primary root growth is largely unclear.

Question: We wanted to know whether ethylene and gibberellin are involved in primary root development in young rice seedlings. What is the crosstalk node between ethylene and gibberellin in primary root growth?

Findings: We show that gibberellins and ethylene successively steer primary root elongation and the subsequent cessation of primary root growth in young rice seedlings. The ethylene signaling transcription factor ETHYLENE INSENSITIVE3-LIKE 1 (OsEIL1) promotes the expression of gibberellin metabolism genes OsGA2ox1, OsGA2ox2, OsGA2ox3, and OsGA2ox5, resulting in the deactivation of gibberellin, which further inhibits cell proliferation in root meristems, and the cessation of primary root growth. Our results shed light on the molecular mechanism of ethylene action during primary root elongation in young rice seedlings, providing insight into the coordination of ethylene and gibberellin during root development and seedling establishment.

Next steps: We aim to improve crop yields by improving their root systems. Further study will focus on how plants perceive external changes and translate cues into adaptive responses by modulating endogenous hormone crosstalk dynamics.

primary root growth, in which the primary root grows rapidly for 7–10 days after germination and then stops growing (Wang et al., 2011; Marcon et al., 2013; Rogers and Benfey, 2015). The growth of the primary root in cereal crops is fundamental for seedling establishment and grain yield (Qin et al., 2019); however, the underlying mechanisms determining growth rate and final length of the primary root are unclear.

The rate of cell proliferation within the root apical meristem is a prime factor affecting root tip growth (Li et al., 2015, 2017). Accumulating evidence indicates that ethylene can inhibit root growth by reducing cell proliferation (Street et al., 2015; Qin et al., 2019; Yoon et al., 2020). The primary root of rice plants emerges and grows in heterogeneous soil, encountering mechanical stress during soil penetration and path formation in the direction of gravitational pull (Correa et al., 2019; Taylor et al., 2021). Intensive investigations show that soil impedance increases ethylene biosynthesis and compacted soil restricts diffusion of ethylene (Okamoto and Takahashi, 2019; Pandey et al., 2021), implying that ethylene-mediated inhibition of cell proliferation in the root apical meristem is essential for primary root growth in response to soil compaction.

Several phytohormones have been shown to act downstream of ethylene to inhibit primary root growth, including auxin and abscisic acid (ABA) (Ma et al., 2014; Yin et al., 2015; Qin et al., 2017). Among the reported hormones, exogenous application of gibberellin (GA) promotes primary root growth, whereas disruption of GA biosynthesis inhibits cell proliferation in the root apical meristem and primary root growth (Li et al., 2015; Lee and Yoon, 2018). The crosstalk between ethylene and GA has been demonstrated in several studies. In *Arabidopsis thaliana*, the loss-of-function of DELLA proteins leads to the reduced sensitivity of roots to ethylene and GA treatment substantially overcomes the inhibition of seedling root growth by the ethylene precursor 1-aminocyclopropane-1-carboxylic acid (ACC) (Achard et al., 2003). Moreover, GA and ethylene cooperatively regulate apical hook curvature by inducing the expression of *HOOKLESS 1* (*HLS1*) via derepressing ETHYLENE INSENSITIVE3 (EIN3)/EIN3-LIKE1 (EIL1) activity (An et al., 2012). In rice, OsEIL1, a master transcriptional regulator of ethylene signaling, transcriptionally activates *SEMIDWARF1* (*SD1*) to promote GA biosynthesis, thereby promoting internode elongation to help plants escape from flooding (Kuroha et al., 2018). These findings indicate that the interaction of ethylene with GA regulates plant development in response to environmental stimuli. In addition to these studies, transcriptome data from the root of *eil1* indicate that some genes involved in GA biosynthesis and catabolic pathways are regulated by OsEIL1 (Yang et al., 2015). Considering that ethylene inhibits, while GA promotes primary root growth (Lee and Yoon, 2018; Qin et al., 2019), we hypothesize that ethylene may reduce endogenous GA content by OsEIL1-mediated transcriptional regulation, thereby inhibiting cell proliferation in the root apical meristem in young rice seedlings.

Here, we report that the ethylene signaling transcription factor OsEIL1 promotes the expression of the GA metabolism genes *OsGA2ox1*, *OsGA2ox2*, *OsGA2ox3*, and *OsGA2ox5*, resulting in the deactivation of GA, which further inhibits cell proliferation in root meristems, and the cessation of primary root growth. Our results shed light on the molecular mechanism of ethylene action during primary root elongation in young rice seedlings, providing insight into the coordination of ethylene and GA during root development and seedling establishment.

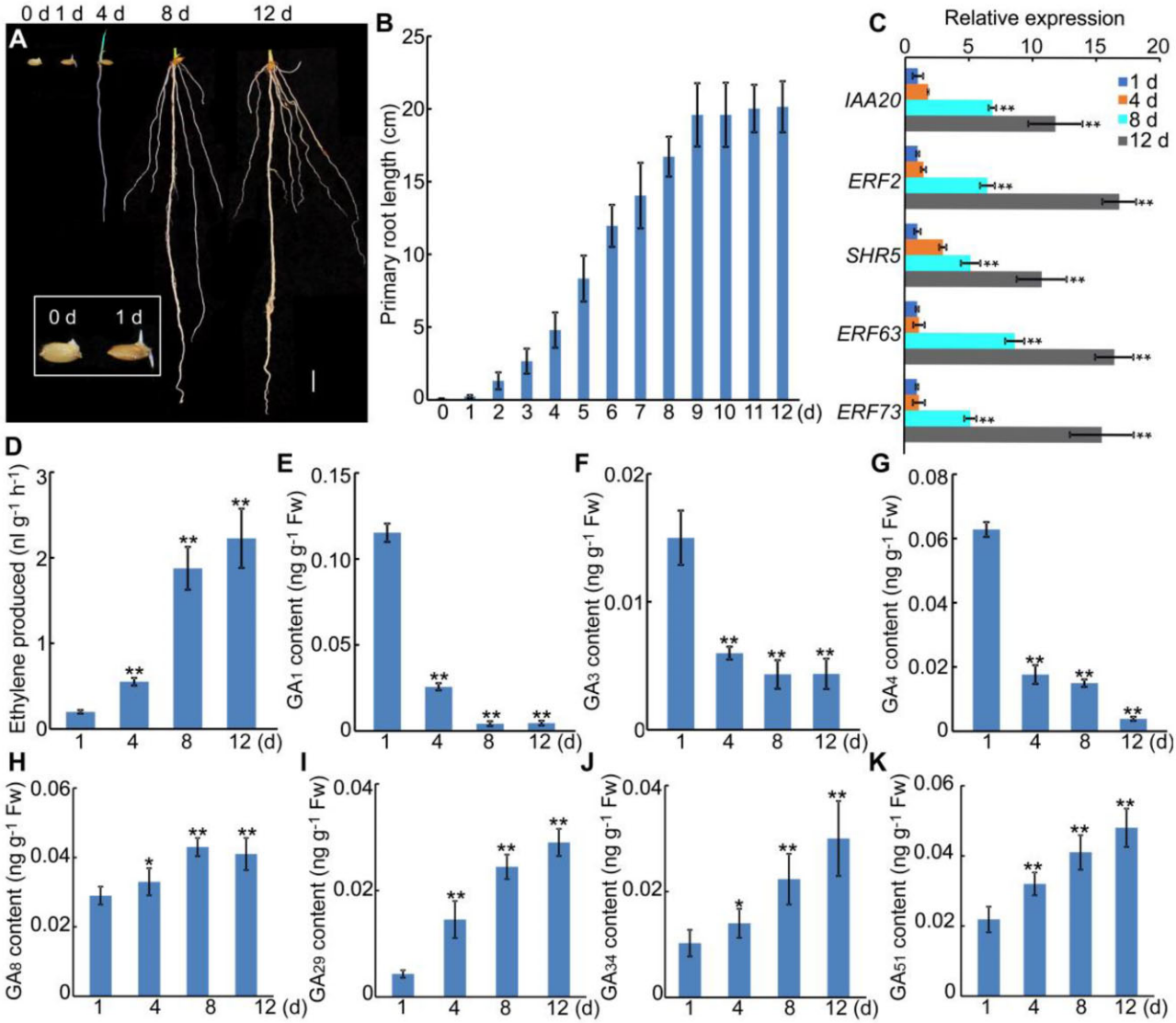

Figure 1 Ethylene and GA are involved in primary root development in young rice seedlings. A, Root phenotypes at different stages of seedling development in soil. Inset shows an enlargement of 0 and 1 days seedlings. Scale bar, 1 cm. B, Primary root length of seedlings at the indicated number of days after imbibition and sprouting. The data are shown as mean ± SD; $n \geqslant 20$ independent seedlings. C, Expression of ethylene-responsive genes in roots at the indicated number of days after imbibition and sprouting relative to *OsActin1*. D, Ethylene production by the roots of 1-, 4-, 8-, and 12-day-old seedlings. E–K, Contents of different GAs in the roots of 1-, 4-, 8-, and 12-day-old seedlings. Fw, fresh weight. For C–K, the data are shown as mean ± SD; $n = 3$ biological replicates. Asterisks indicate significant differences compared with 1-day-old seedlings at $^{*}P < 0.05$ and $^{**}P < 0.01$ (Student's *t* test). d, days after seed imbibition in water and sprouting.

Results

Ethylene and GA orchestrate primary root growth in young rice seedlings

As an important belowground plant organ, the root system mediates water and nutrient uptake and provides mechanical support for shoot growth (Shekhar et al., 2019). As primary root growth is essential and fundamental for seedling establishment and improvement of grain yield (Qin et al., 2019), we first examined primary root growth in wild-type Nipponbare (Nip) seedlings to determine the key developmental time points. The primary root protruded through the seed coat at 1 day (after seed imbibition in water and sprouting), began rapid growth at 3–4 days, the length plateaued at 8–9 days, and stopped growing at 12 days (Figure 1, A and B). We thus used 1, 4, 8, and 12 days as key time points for our analyses.

Emerging reports have evidenced that soil impedance and compaction as the primary root penetrates the soil can lead to the accumulation of ethylene in the root (Okamoto and Takahashi, 2019; Pandey et al., 2021). Therefore, we speculate that ethylene might be involved in regulating primary root development in young rice seedlings. To uncover the role of ethylene in primary root development, we measured the expression of ethylene-responsive genes and the level of

ethylene biosynthesis in roots at these four developmental stages. Expression of ethylene-responsive genes increased significantly during primary root growth (Figure 1C), as did ethylene production (Figure 1D), confirming that ethylene is a regulator of root growth in young rice seedlings.

As ethylene interacts with phytohormone signals (Ma et al., 2014; Yin et al., 2015; Qin et al., 2017) and GA promotes primary root growth (Ubeda-Tomas et al., 2009; Li et al., 2015; Lee and Yoon, 2018), we examined whether GA levels also changed during root growth. Levels of bioactive GAs (GA_1, GA_3 and GA_4) gradually decreased and levels of inactive GAs (GA_8, GA_{29}, GA_{34} and GA_{51}) gradually increased, over the 12 days (Figure 1, E–K), revealing that homeostasis of ethylene and GA may be coordinated to regulate primary root growth in young rice seedlings.

GA is required for ethylene-inhibited cell proliferation in the root apical meristem

Considering that the primary root was growing rapidly at 4 days and ethylene and GA levels changed dramatically at this time point, we selected this time point for further analyses. The root growth rate corresponds with the cell number in the root meristem, as this determines the number of cells that can differentiate at a given time (Street et al., 2015; Vaseva et al., 2018; Yamada et al., 2020). To investigate whether ethylene inhibits primary root growth by affecting cell proliferation in the root meristem, we treated Nip and ethylene-insensitive mutants *ein2* and *eil1* (Ma et al., 2013; Yang et al., 2015) with ethylene and measured the cell number and size of the primary root meristem (Street et al., 2015; Yamada et al., 2020). OsEIN2 is a central component of ethylene signaling in rice. Mutation in *OsEIN2* leads to ethylene insensitivity both in the roots and coleoptiles (Ma et al., 2013). Rice has six EIL1 homologs, designated as OsEIL1 to OsEIL6. OsEIL1 and OsEIL2 showed the highest similarity to *Arabidopsis* EIN3, which is the master transcriptional regulator of ethylene signaling. Disruption of *OsEIL1* caused ethylene insensitivity mainly in the roots, whereas silencing of *OsEIL2* led to ethylene insensitivity mainly in the coleoptiles of etiolated seedlings. OsEIL3 and OsEIL4 have no significant effects on the ethylene response in plants; OsEIL5 and OsEIL6 lack transcriptional activation abilities (Yang et al., 2015). In this study, we mainly focused on the regulation of ethylene on primary root development; thus, we chose OsEIL1 for further research. In Nip roots, ethylene treatment reduced the meristem size (by ~35%) and the cortical cell number (by ~30%), whereas the cortical cell diameter increased (by ~40%; Supplemental Figure S1), consistent with previous reports (Street et al., 2015; Pandey et al., 2021). The roots of *ein2* and *eil1* mutants did not respond to ethylene treatment (Supplemental Figure S1), confirming that the ethylene signaling pathway is required to inhibit cell proliferation in root meristems and promote radial expansion of cortical cells in the elongation zone.

Studies have shown that GA plays an important role in regulating cell proliferation in root growth (Ubeda-Tomas et al., 2009; Li et al., 2015). The dramatic changes of ethylene and GA in the developmental processes of primary root growth suggest that GA might be involved in ethylene-inhibited cell proliferation in the root meristem. To explore whether GA is associated with ethylene-inhibited cell proliferation in root meristems, we treated Nip seedlings with ethylene in the presence of GA_3. Ethylene treatment significantly inhibited root elongation, whereas exogenous GA_3 treatment slightly promoted root elongation, and substantially overcame the ethylene-inhibited root elongation (Figure 2A). There are two possible explanations for this observation. First, ethylene and GA work in parallel to regulate root elongation. Second, GA is required for ethylene-inhibited root elongation. To further investigate the above explanations, we analyzed the ethylene response in the rice DELLA protein mutant *slender rice 1* (*slr1*), which exhibits a constitutive GA response (Ikeda et al., 2001). In the absence of ethylene, wild-type and *slr1* seedling root lengths were statistically indistinguishable (Supplemental Figure S2). When the plants were exposed to exogenous ethylene treatment, the root growth of wild type and *slr1* was inhibited, but *slr1* was more resistant than the wild type to the effects of ethylene (Supplemental Figure S2), indicating that SLR1-mediated GA signaling is partially required to inhibit primary root growth via ethylene, and ethylene also inhibits root elongation via a SLR1-independent pathway.

To further prove that GA is required for ethylene-inhibited root elongation, we measured the content of GA in roots. The results showed that bioactive GA levels were higher in *ein2* and *eil1* roots than in those of Nip, whereas levels of inactive GAs were significantly reduced in ethylene-insensitive roots. By contrast, bioactive GA levels were lower, and inactive GA levels were higher, in roots overexpressing *OsEIN2* or *OsEIL1* (*EIN2-OX*, *EIL1-OX*) (Figure 2B), indicating that GA signaling is involved in ethylene-mediated root growth. Further treatment with paclobutrazol (PAC, a GA biosynthesis inhibitor) showed that 0.1 μM PAC treatment completely rescued the longer root phenotype of *ein2* and *eil1* plants (Figure 2, C and D), and this concentration had no obvious inhibitory effects on root growth in Nip seedlings. Similarly, exogenous application of 1 μM GA_3 did not affect Nip roots, but largely restored the short and twisted *EIN2-OX* and *EIL1-OX* primary roots to a normal phenotype (Figure 2, E and F). Microscopy analysis of root tip longitudinal sections further demonstrated that 0.1 μM PAC treatment did not affect Nip but caused the reduction of meristem size and cortical cell number in *ein2* and *eil1* primary roots, mimicking the effect of ethylene treatment on Nip roots (Figure 3, A, C, and D). Conversely, root meristem size and cortical cell number were increased in *EIN2-OX* and *EIL1-OX* plants after 1 μM GA_3 treatment, and this concentration had no obvious effects on Nip seedlings (Figure 3, B, E, and F), demonstrating that GA acts downstream of ethylene signaling to modulate cell proliferation in the root meristem.

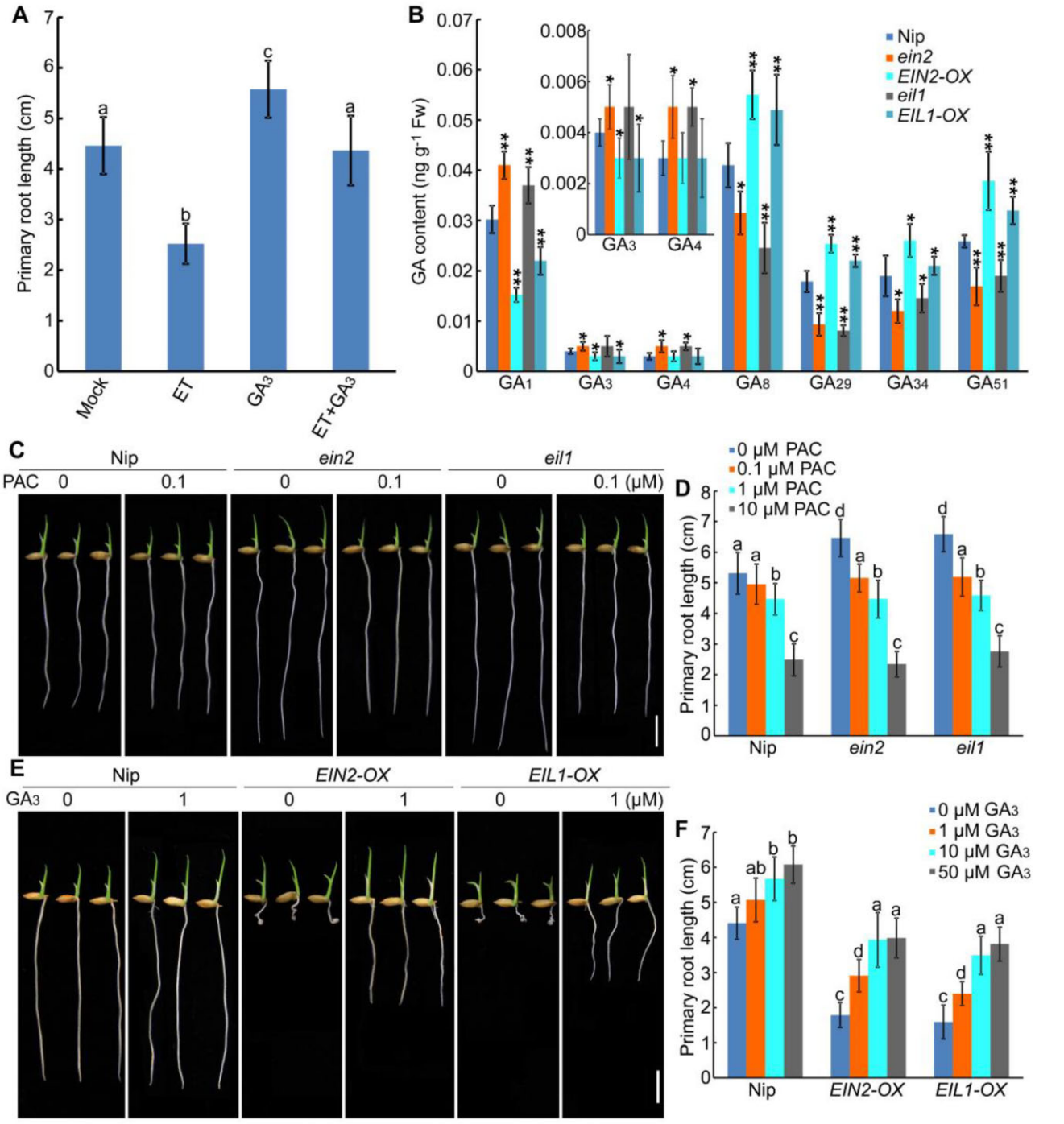

Figure 2 GA is required for ethylene-modulated root elongation. A, Primary root length of 4-day-old seedlings grown in the absence (mock) or presence of 10 μL/L ethylene (ET), 1 μM GA_3, or 10 μL/L ET plus 1 μM GA_3. The data are shown as mean ± SD; n = 20–30 independent seedlings. Different letters indicate significant differences ($P < 0.05$, one-way ANOVA with Tukey's test). B, Content of various GAs in the roots of 4-day-old Nip and *OsEIN2* and *OsEIL1* knockout and OX seedlings. Inset graph shows an enlargement of GA_3 and GA_4 content. The data are shown as mean ± SD; n = 3 biological replicates. The P-values indicate significant differences from Nip using a Student's t test at $^*P < 0.05$; $^{**}P < 0.01$. Fw, fresh weight. C, Phenotypes of the primary roots of 4-day-old Nip, *ein2*, and *eil1* seedlings with or without 0.1 μM PAC treatment. Scale bar, 1 cm. PAC, paclobutrazol. D, Primary root length of 4-day-old Nip, *ein2*, and *eil1* seedlings with 0, 0.1, 1, or 10 μM PAC treatment. E, Phenotypes of the primary roots of 4-day-old Nip, *EIN2-OX*, and *EIL1-OX* seedlings with or without 1 μM GA_3 treatment. Scale bar, 1 cm. F, Primary root length of 4-day-old Nip, *EIN2-OX*, and *EIL1-OX* seedlings with 0, 1, 10, or 50 μM GA_3 treatment. For (D) and (F), the data are shown as mean ± SD; $n \geqslant 20$ independent seedlings. Different letters indicate significant differences ($P < 0.05$, one-way ANOVA with Tukey's test).

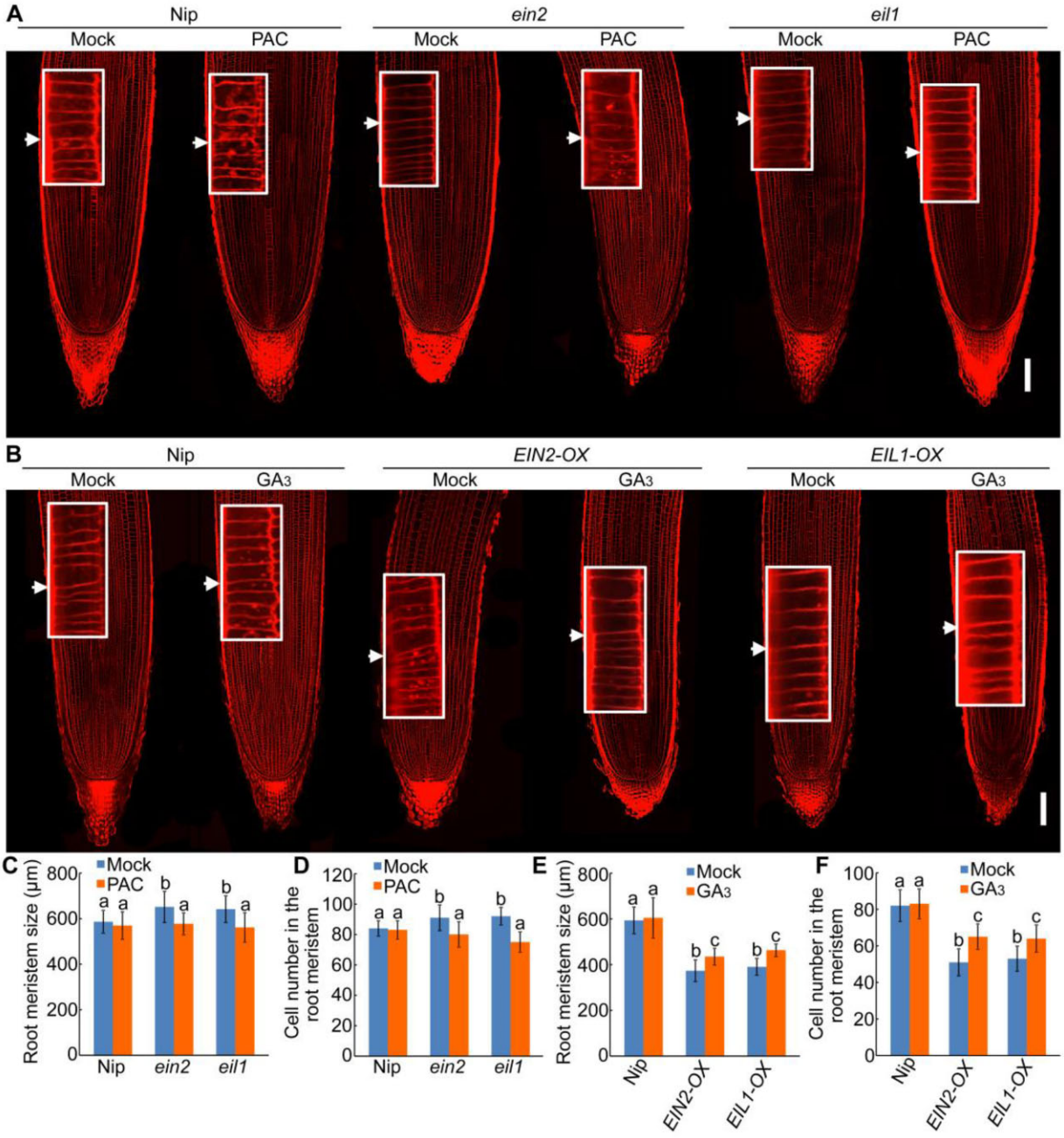

Figure 3 Exogenous GA_3 or PAC treatment rescues the root phenotypes of plants with altered ethylene signaling. A and B, Longitudinal sections of root tips of 4-day-old Nip, and *OsEIN2* and *OsEIL1* knockout and OX seedlings treated with ethanol (mock) and 0.1 μM PAC or 1 μM GA_3. White arrows indicate the proximal end of the root meristem; inset shows an enlargement (four times magnification) of the region at the proximal end of the root meristem. Scale bars, 100 μm. C–F, Length (C) and (E) and cortical cell number (D) and (F) of the root meristem zones of seedlings exemplified in (A) and (B). The data are shown as mean ± SD; $n \geqslant 10$ independent seedlings. Different letters indicate significant differences ($P < 0.05$, one-way ANOVA with Tukey's test).

OsEIL1 directly activates the transcription of *OsGA2ox* genes

Crosstalk between ethylene and GA signaling has been reported in several studies (Achard et al., 2003; An et al., 2012; Kuroha et al., 2018); for example in deepwater rice, ethylene-induced expression of *SD1*, which encodes a GA biosynthetic enzyme, is affected by direct binding of OsEIL1 to the *SD1* promoter (Kuroha et al., 2018). Our data on the levels of active and inactive GAs in *eil1* and *ein2* mutants suggest that ethylene may activate genes involved in GA catabolism to cause GA inactivation. As inactivation of GA_1, GA_3, and GA_4 is catalyzed by GA2-oxidases (GA2ox) (Sakai et al., 2003; Lo et al., 2008), we then examined the expression patterns of *OsGA2ox* genes in RNA sequencing data from *ein2* and *eil1* roots (SRP041468) (Yang et al., 2015) and found that *OsGA2ox3* is regulated by both OsEIN2 and

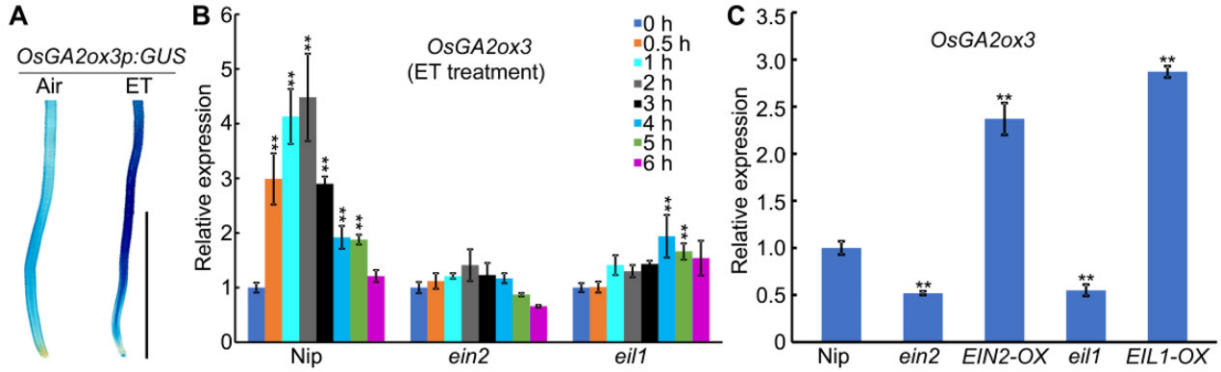

Figure 4 Ethylene-induced *OsGA2ox3* expression depends on the ethylene signaling pathway. A, GUS activity in the roots of 4-day-old transgenic seedlings harboring the *OsGA2ox3pro:GUS* expression construct with and without 10 μL/L ethylene (ET) treatment for 6 h. Scale bar, 1 cm. B, Expression of *OsGA2ox3* in the roots of 4-day-old Nip, *ein2*, and *eil1* seedlings over 6 h during 10 μL/L ethylene treatment relative to *OsActin1*. C, Expression of *OsGA2ox3* in the roots of 4-day-old Nip, *ein2*, *EIN2-OX*, *eil1*, and *EIL1-OX* seedlings relative to *OsActin1*. For (B) and (C), the data are shown as mean ± SD; $n = 3$ biological replicates. Asterisks indicate significant differences compared with 0 h (B) or Nip (C) values at $^{**}P < 0.01$ (Student's *t* test).

OsEIL1. *OsGA2ox3* promoter activity and gene expression in response to ethylene were confirmed by β-glucuronidase (GUS) reporter activity and quantitative real-time PCR (qPCR) analyses (Figure 4, A–C), suggesting that ethylene promotes GA inactivation, possibly by activating the expression of *OsGA2ox3*, and implying that *OsGA2ox3* is a potential target of OsEIL1.

To determine whether OsEIL1 functions as a direct regulator of *OsGA2ox3*, we analyzed the promoter sequence of *OsGA2ox3* and identified four sites predicted to bind OsEIL1 (Yang et al., 2015; Figure 5A). Hence, we performed a chromatin immunoprecipitation (ChIP) assay using transgenic plants harboring myc-tagged OsEIL1 (OsEIL1-myc). As shown in Figure 5B, anti-myc antibodies precipitated the P1 and P3 fragments of the *OsGA2ox3* promoter. This interaction was further confirmed by qPCR performed using the same ChIP products and PCR primers flanking EIL1 binding sites (EBS) in the *OsGA2ox3* promoter (Figure 5C). Subsequently, we conducted an electrophoretic mobility shift assay (EMSA) with GST-EIL1-N fusion protein expressed in *Escherichia coli*. As shown in Figure 5D, the GST-EIL1-N fusion protein directly bound to DNA probes containing the EBS motif, which is present in the P1 and P3 fragments of the *OsGA2ox3* promoter, but it did not bind to the DNA probes with mutated EBS motif. The specificity of this binding was confirmed by a competition assay using unlabeled competitor probe (Figure 5D). These results indicate that OsEIL1 directly binds to the *OsGA2ox3* promoters in vitro and in vivo.

To determine whether OsEIL1 activates the expression of *OsGA2ox3*, we performed a transient expression assay in which we fused the 2,600-bp promoter sequence upstream of the ATG codon of *OsGA2ox3* to the *LUCIFERASE* (*LUC*) reporter gene and cotransfected tobacco leaves and rice protoplasts with the effector plasmid harboring *35Spro:EIL1*. The presence of the effector significantly increased LUC activity driven by the *OsGA2ox3* promoter compared with the control vector (Figure 5E and Supplemental Figure S3). This activation was further confirmed by the mutated *OsGA2ox3* promoter (Figure 5E). Compared with the intact *OsGA2ox3* promoter, the mutation of the EBS in the P1 or P3 fragment slightly reduced the LUC activity, whereas the mutation of the EBS in the P2 fragment did not affect LUC activity, when all the EBS in the *OsGA2ox3* promoter were mutated, the activation of OsEIL1 on *OsGA2ox3* was completely abolished (Figure 5E). These results indicate that the EBS in the P1 and P3 fragments is essential for OsEIL1 to activate the expression of *OsGA2ox3*.

Previous studies have shown that rice has 10 *OsGA2ox* genes (Lo et al., 2008). To investigate whether other *OsGA2ox* genes are also regulated by OsEIL1, we detected the expression of *OsGA2ox* genes in *OsEIN2* and *OsEIL1* mutants and overexpressing seedling roots, and found that *OsGA2ox1*, *OsGA2ox2*, *OsGA2ox5*, and *OsGA2ox10* were also regulated by OsEIN2 and OsEIL1 (Supplemental Figure S4A). ChIP-qPCR analysis showed that OsEIL1 bound to the promoters of *OsGA2ox1*, *OsGA2ox2*, and *OsGA2ox5* in vivo (Supplemental Figure S4, B and C). These findings indicate that *OsGA2ox1*, *OsGA2ox2*, *OsGA2ox3*, and *OsGA2ox5* may be involved in ethylene-inhibited root elongation.

OsGA2ox3 overexpression alters cell proliferation and the ethylene response in the primary root

To investigate the roles of *OsGA2ox3* in root growth, we generated overexpression (OX) lines containing the coding region of *OsGA2ox3* under the control of the CaMV35S promoter. The increased expression of the target gene was confirmed by qPCR (Supplemental Figure S5, A and B). We also generated loss-of-function mutants of *OsGA2ox3* (*osga2ox3*) via CRISPR-Cas9, as confirmed by sequencing the target gene. The *osga2ox3-1*, *osga2ox3-2*, and *osga2ox3-3* knockout lines contained 1-bp insertions in coding regions of the target gene, leading to a frame shift in the open-reading frame and the generation of a premature stop codon

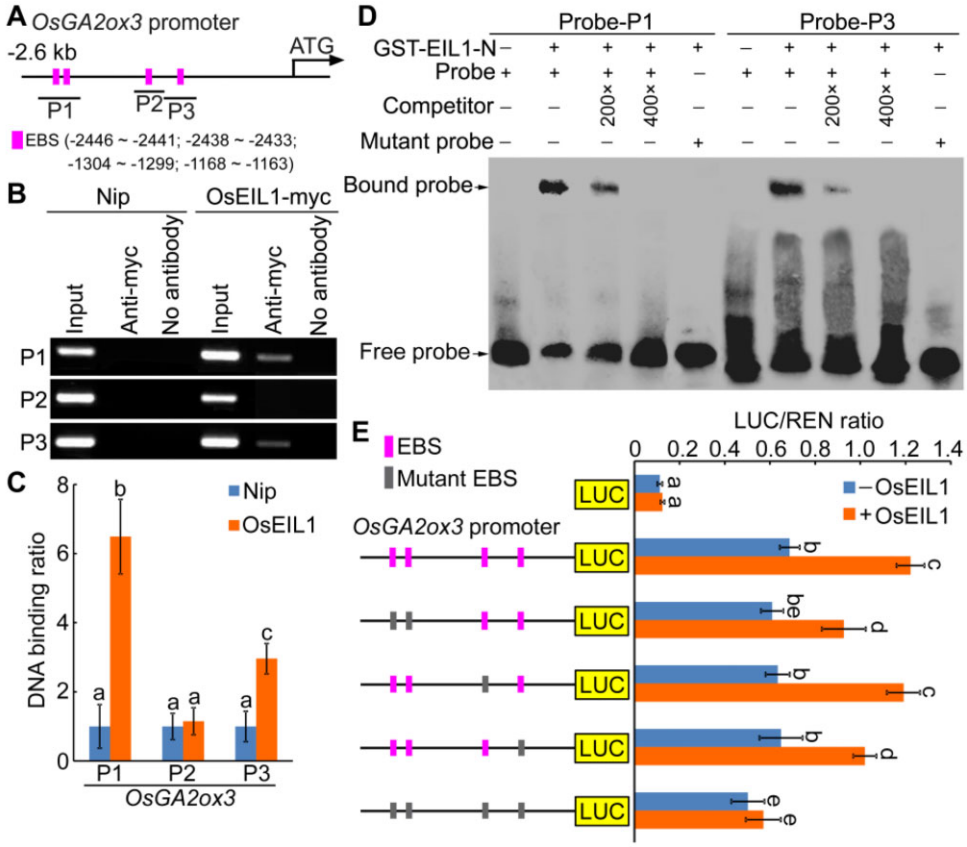

Figure 5 OsEIL1 directly binds to the promoter of *OsGA2ox3* to activate its expression. A, Schematic diagram of putative EBS (ATGTA/TACAT) in the *OsGA2ox3* promoter. P1–P3 are the *OsGA2ox3* promoter fragments used in ChIP and EMSA experiments. The pink boxes indicate putative EBS and the black lines indicate the promoter sequence. B, Anti-myc ChIP assays using DNA from the roots of 4-day-old Nip seedlings and seedlings overexpressing myc-tagged *OsEIL1* (OsEIL1-myc). C, Enrichment fold of the ChIP-PCR signals from the regions shown in (A) determined by qPCR. The data are shown as mean ± SD; $n = 3$ biological replicates. Different letters indicate significant differences ($P < 0.05$, one-way ANOVA with Tukey's test). D, EMSA using normal (ATGTA/TACAT) and mutated EBS (GGAGC) in P1 and P3 with glutathione-*S*-transferase-tagged OsEIL1 N-terminal fusion protein (GST-EIL1-N). GST-tag was used in place of GST-EIL1-N for no-protein controls. Protein was incubated with biotin-labeled DNA fragments (Probe), tested for competition by adding an excess of unlabeled probe (Competitor), and for specificity with labeled mutant probe. Three biological replicates were performed, with similar results. E, Dual-LUC assay results from transient transformation of rice mesophyll protoplasts with constructs constitutively expressing EIL1 and/or the LUC reporter gene under control of the intact *OsGA2ox3* promoter or mutant *OsGA2ox3* promoter. Pink frame represents normal EBS (ATGTA/TACAT) and gray frame represents mutated EBS (GGAGC). The data are shown as mean ± SD; $n = 3$ biological replicates. Different letters indicate significant differences ($P < 0.05$, one-way ANOVA with Tukey's test).

(Supplemental Figure S5, C–E). OX of *OsGA2ox3* leads to a significant decrease in plant height, with higher levels of expression corresponding to shorter plants (Supplemental Figure S5F). Loss-of-function mutant plants were similar in plant height to wild type (Supplemental Figure S5F), likely due to functional redundancy of OsGA2ox proteins in GA inactivation. Primary root length was also significantly reduced in the *OsGA2ox3-OX* lines, but not in the *osga2ox3* knockout seedlings (Figure 6, A–D).

To further study the function of *OsGA2ox3* in the root ethylene response, we examined the root length of *OsGA2ox3* OX and knockout seedlings after ethylene treatment. With exogenous ethylene treatment, the inhibition of root growth of the *OsGA2ox3-OX* lines was more severe than that of the wild type (Figure 6, A and B), indicating that overexpressing *OsGA2ox3* enhances the ethylene response in the roots. Correspondingly, the roots of the *osga2ox3* mutants exhibited reduced sensitivity to ethylene (Figure 6, C and D), indicating that the OsGA2ox3-mediated pathway is partially required for the regulation of the ethylene-induced inhibition of root growth. Subsequently, we measured the GA content in the *osga2ox3* mutant and *OsGA2ox3-OX* seedling roots with or without ethylene treatment. OX of *OsGA2ox3* caused a significant decrease in bioactive GA levels and an increase in inactive GA levels in roots, whereas *osga2ox3* mutants showed a similar GA contents as the wild type in the absence of ethylene (Figure 6, E and F), further demonstrating the functional redundancy of OsGA2ox proteins in GA inactivation. Ethylene treatment significantly reduced bioactive GA levels and increased inactive GA levels in wild-type roots (Figure 6, E and F). This effect was weakened in *osga2ox3* mutant roots, but enhanced

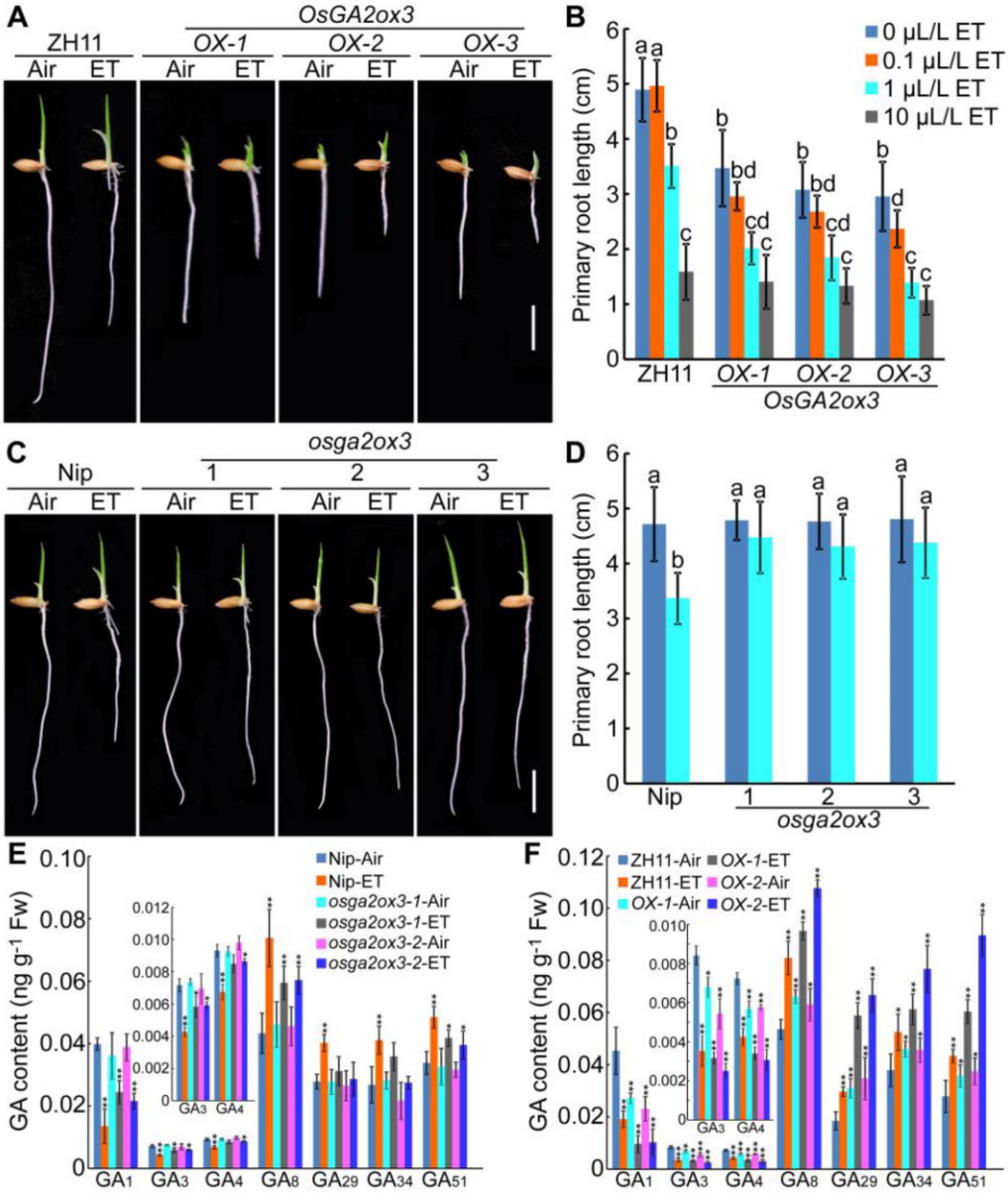

Figure 6 Ethylene-inhibited primary root elongation is partially dependent on OsGA2ox3-mediated GA deactivation. A and C, Phenotypes of the primary roots of 4-day-old wild-type and *OsGA2ox3* OX and knockout seedlings with or without 1 μL/L ethylene (ET) treatment. Scale bar, 1 cm. B and D, Primary root length of 4-day-old wild-type and *OsGA2ox3* OX and knockout seedlings treated with various concentrations of ethylene. The data are shown as mean ± SD; $n \geqslant 20$ independent seedlings. Different letters indicate significant differences ($P < 0.05$, one-way ANOVA with Tukey's test). E and F, Content of various GAs in the roots of 4-day-old Nip, *osga2ox3* mutants, and *OsGA2ox3* OX seedlings in the absence or presence of ethylene. Four-day-old seedlings were treated with or without 10 μL/L ethylene for 24 h. Inset graph shows an enlargement of GA_3 and GA_4 content. The data are shown as mean ± SD; $n = 3$ biological replicates. The *P*-values indicate significant differences from Nip-Air or ZH11-Air using a Student's *t* test at $^*P < 0.05$; $^{**}P < 0.01$. Fw, fresh weight.

in *OsGA2ox3-OX* seedling roots (Figure 6, E and F). These results indicate that ethylene-inhibited primary root elongation is partially dependent on OsGA2ox3-mediated GA deactivation.

As root development is highly modulated by the physical properties of soil, we also examined the soil-grown root phenotype of *osga2ox3* and *OsGA2ox3-OX* plants. Computed tomography (CT) imaging confirms that a similar effect was observed in soil, showing that the primary root of *OsGA2ox3-OX* was much shorter than that of the wild type or *osga2ox3* (Figure 7, A and B). Anatomical analysis of root apices further demonstrated that *OsGA2ox3* OX significantly reduced root meristem size (by ~16%–23%) and cortical cell number (by ~10%–17%), but again, no obvious difference was observed between the loss-of-function mutants and the wild type (Supplemental Figure S6). These results together suggest that *OsGA2ox3* OX leads to a decrease in bioactive GAs in roots, thereby inhibiting the cell

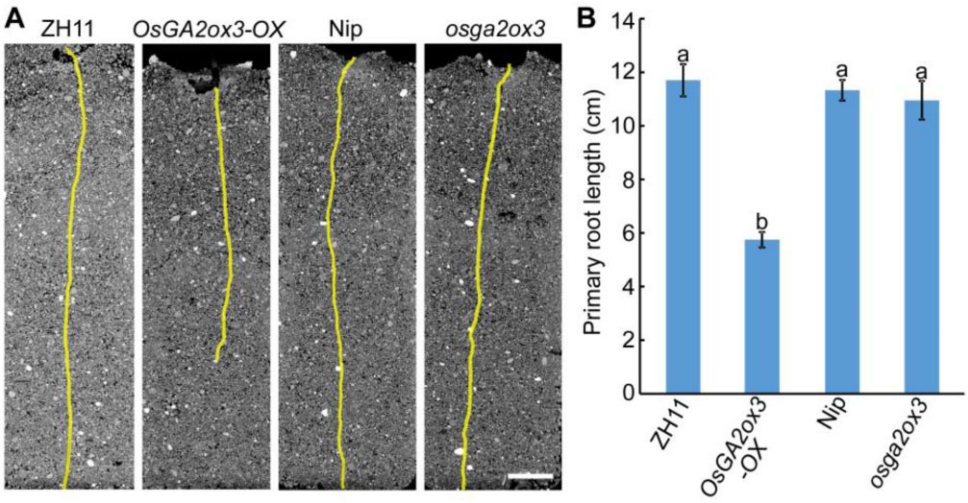

Figure 7 Transgenic lines overexpressing *OsGA2ox3* displayed inhibited root growth in soil conditions. A, Representative CT images of the roots of 5-day-old *OsGA2ox3* OX and *osga2ox3* knockout lines compared with their respective wild-type lines in soil. Scale bar, 1 cm. B, Length of primary roots of plants exemplified in (A). The data are shown as mean ± SD; $n \geqslant 5$ independent seedlings. Different letters indicate significant differences ($P < 0.05$, one-way ANOVA with Tukey's test).

proliferation in the root meristem and root elongation and also impacts plant height, likely through an associated physiological pathway in shoot development related to the *SD1*-mediated semi-dwarf phenotype.

OsGA2ox3 functions downstream of OsEIL1 to regulate cell proliferation and root growth

To explore the genetic relationship between OsGA2ox3 and the ethylene signaling transcription factor OsEIL1, we generated double mutant lines with different combinations of genetic loss-of-function or OX. Loss of *OsGA2ox3* in *eil1* mutants had no effect on the *eil1* primary root length or meristem size (Figure 8, A and B and Supplemental Figure S7). Compared with the highly shortened *EIL1-OX* roots, *osga2ox3 EIL1-OX* primary root was slightly longer, with larger root meristems and higher cortical cell numbers (Figure 8, A and B and Supplemental Figure S7), indicating that the effect of ethylene on root growth occurs through multiple pathways, of which the *OsGA2ox3*-mediated pathway is one. The primary root in *OsGA2ox3-OX eil1* seedlings was significantly shorter than that in wild type and *eil1*, but similar to that in *OsGA2ox3-OX* seedlings (Figure 8, A and B). Anatomical analysis of root apices revealed that the root meristem size and cortical cell number of *OsGA2ox3-OX eil1* seedlings were reduced compared with that of wild-type and *eil1* plants but were similar to those of *OsGA2ox3-OX* seedlings (Supplemental Figure S7). These data suggest that OsGA2ox3 acts downstream of the ethylene signaling pathway to regulate cell proliferation and root growth.

Next, we examined the above genetic relationship under ethylene treatment. Upon exposure to ethylene, the roots of the *osga2ox3 eil1* and *OsGA2ox3-OX eil1* seedlings displayed an absolute insensitivity to exogenous ethylene (Figure 8, A and B), indicating that OsEIL1 and OsGA2ox3 most likely act within the same pathway for ethylene-induced root inhibition, and the root ethylene response of *OsGA2ox3-OX* requires OsEIL1. Further analysis of the ethylene response of the *osga2ox3 EIL1-OX* seedlings showed that the inhibition of root growth of *EIL1-OX* seedlings was partially alleviated in the *osga2ox3 EIL1-OX* seedlings (Figure 8, A and B), indicating that the OsGA2ox3-mediated pathway is partially required by OsEIL1 signaling for the regulation of the ethylene-induced inhibition of root growth.

Discussion

Rice is a staple food for more than half of the world population. Improving the rice root system is one of the most important approaches to increase grain yield in adverse conditions. The rice primary root develops shortly after germination and is critical for seedling establishment (Marcon et al., 2013) and root growth requires the successive formation of new cells from the root meristem (Yoon et al., 2020). Thus, root meristem activity is the most critical process influencing root development. Previous studies have shown that ethylene plays an important role in controlling meristem activity through restricting cell proliferation in the root meristem (Street et al., 2015; Yoon et al., 2020). In the present study, we have provided evidence that the cooperation of ethylene and GA homeostasis steers primary root development in young rice seedlings. We have demonstrated that the ethylene signaling transcription factor OsEIL1 directly activates the expression of the GA metabolism genes *OsGA2ox1*, *OsGA2ox2*, *OsGA2ox3*, and *OsGA2ox5*, which further controls cell proliferation in the root meristem and primary root elongation. Thus, our data reveal that OsGA2ox3 is a novel node in the crosstalk between ethylene and GA metabolism during root development.

As the belowground organ of the plant, root system architecture is shaped by soil bio-physico-chemical properties (Shekhar et al., 2019; Pandey et al., 2021). Soil compaction is

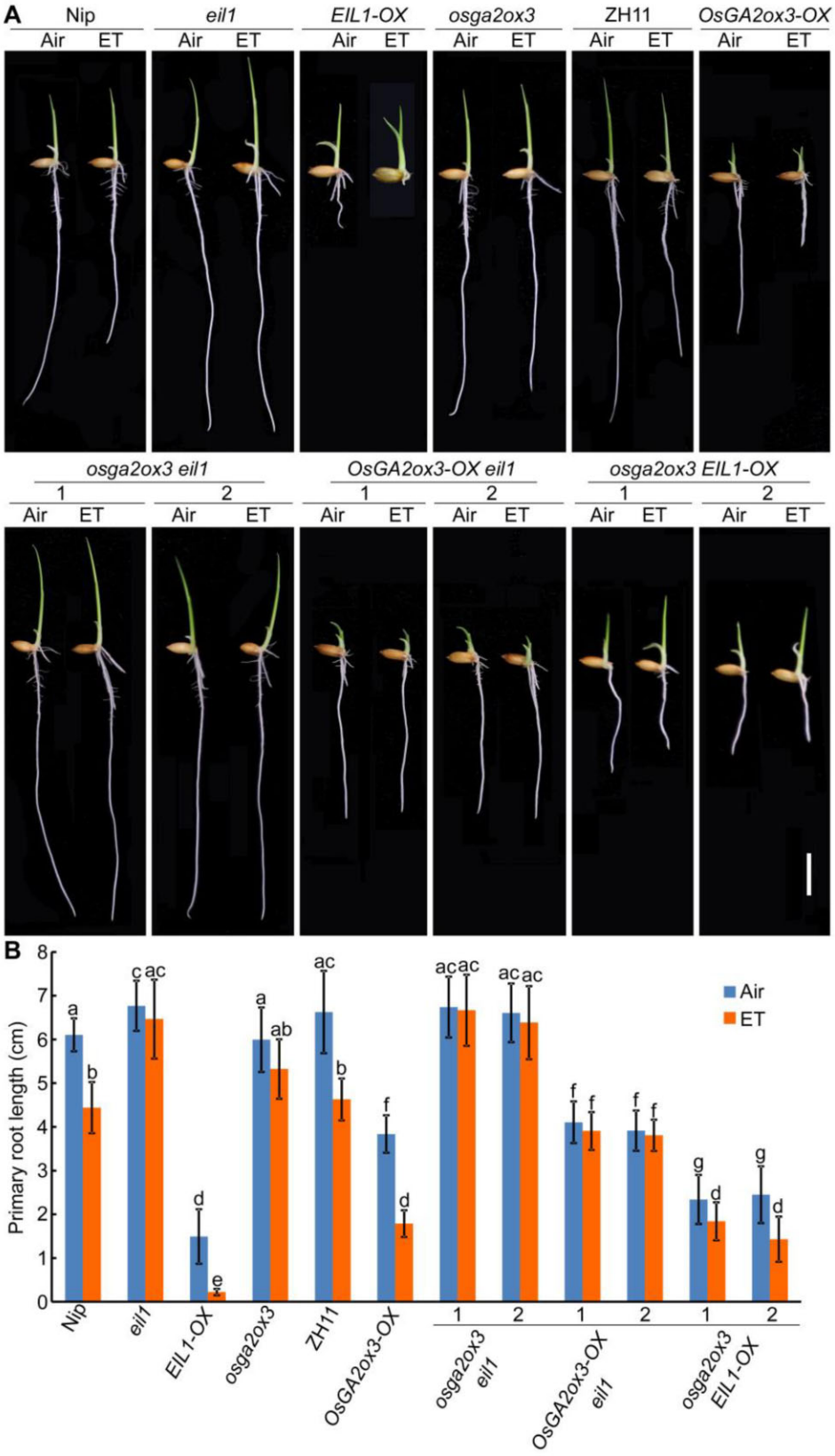

Figure 8 OsGA2ox3 acts downstream of OsEIL1 to regulate ethylene response in roots. A, Phenotypes of the primary roots of 4-day-old wild-type and combinations of *OsGA2ox3* and *OsEIL1* knockout and OX seedlings with or without 1 μL/L ethylene (ET) treatment. Scale bar, 1 cm. B, Primary root length of seedlings exemplified in (A). The data are shown as mean ± SD; $n \geqslant 20$ independent seedlings. Different letters indicate significant differences ($P < 0.05$, one-way ANOVA with Tukey's test).

a significant problem on a global scale, constraining crop productivity through restriction of root growth and exploration in deeper soil profiles, which in turn limits access to nutrients and water (Correa et al., 2019). Recent studies have shown that soil compaction inhibits root growth through restricting ethylene diffusion (Pandey et al., 2021). Moreover, rice is a semi-aquatic plant that grows in a water-saturating environment for most of its life cycle; this means that rice roots are also well adapted to growing in hypoxic conditions. Rice is well adapted to hypoxia stress through multiple responses and ethylene acts as a central player in these adaptations (Fukao and Bailey-Serres, 2008; Yukiyoshi and Karahara, 2014; Yamauchi et al., 2017). Under hypoxic conditions, the expression of the ethylene biosynthetic genes and ethylene production in rice roots was stimulated (Yamauchi et al., 2016, 2017). Moreover, the diffusion of ethylene in water is extremely slow ($<10^{-4}$ times) (Hattori et al., 2009), which makes it even more prone to be trapped near root tissues. In the present study, we conclude that ethylene deactivates bioactive GAs, resulting in inhibition of cell proliferation in the root apical meristem, producing a shorter primary root under hydroponic conditions. This effect has also been observed in the soil, where *OsGA2ox3* OX inhibits root growth. The tillage layer in paddy fields is ~15–20 cm thick, which is about the root length of wild-type rice plants in soil. As the roots grow down, the soil compaction and impedance increases, leading to increased local ethylene concentrations, and the accumulation of OsEIL1 (Potocka and Szymanowska-Pulka, 2018; Pandey et al., 2021). Thus, our results indicate that the reduction of bioactive GAs restricts root growth in the soil or water-saturating environment, revealing crosstalk between ethylene and GA during root development and seedling establishment.

Crosstalk between ethylene and GA occurs during various biological processes, such as escaping from submergence, apical hook development, and abiotic and biotic stress responses (Hattori et al., 2009; An et al., 2012; Verma et al., 2016; Kuroha et al., 2018), but it is unclear how ethylene and GA interact during root elongation in young rice seedlings. In *Arabidopsis*, ethylene inhibits the growth of roots via the DELLA proteins and ethylene delays the GA-induced disappearance of the DELLA protein (Achard et al., 2003). In the present study, we demonstrated that ethylene deactivates bioactive GAs by activating the expression of GA metabolism genes *OsGA2ox1*, *OsGA2ox2*, *OsGA2ox3*, and *OsGA2ox5*, which may explain why ethylene can delay the GA-induced disappearance of DELLA protein. In addition, the rice DELLA protein mutant *slr1* exhibited reduced sensitivity to ethylene in roots, indicating that a similar mechanism might exist in rice and *Arabidopsis*. In deepwater rice, submergence induces ethylene accumulation following the stabilization of OsEIL1. OsEIL1 binds to promoters of the *SNORKEL1/2* (*SK1/2*) genes to induce their transcript accumulation, which then triggers remarkable internode elongation via GA (Hattori et al., 2009; Kuroha et al., 2018).

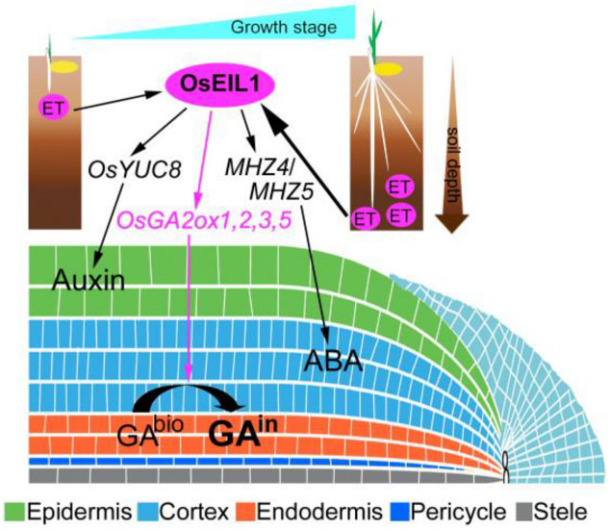

Figure 9 Schematic representation of ethylene roles in coordinating different hormone signals to control/inhibit specific root growth processes. As root growth continues downward, soil impedance and oxygen deficiency activate ethylene production and soil compaction restricts diffusion of ethylene (ET), leading to the accumulation of OsEIL1 in the roots, thus activating *OsYUC8*, *OsGA2ox1*, *OsGA2ox2*, *OsGA2ox3*, *OsGA2ox5*, *MHZ4/ABA4*, and *MHZ5/CRTISO* to promote auxin biosynthesis in epidermal cells and ABA biosynthesis in cortical cells, and inactivating bioactive GAs in endodermal cells, ultimately resulting in the inhibition of cell proliferation in the root meristem and the cessation of primary root growth. GA^{bio}, bioactive GAs; GA^{in}, inactive GAs.

Similarly, OsEIL1 binds to the promoter of *SD1*, and the deepwater rice-specific haplotype (DWH) mediates rapid amplification of *SD1* transactivation, thereby enhancing the synthesis of bioactive GAs to promote internode elongation to help rice escape from flooding (Kuroha et al., 2018). In this study, we demonstrated that ethylene promotes the inactivation of bioactive GAs, resulting in the cessation of primary root growth, which is distinctive from a previous report of the OsEIL1–*SD1* interaction promoting internode elongation in flooding-resistant rice (Kuroha et al., 2018), indicating that different features might exist in different organs.

Previous investigations have demonstrated that OsEIL1 activates the expression of the auxin biosynthesis gene *OsYUC8* or the ABA biosynthetic gene *MHZ4/ABA4* or *MHZ5/CRTISO* to promote auxin and ABA accumulation in roots, respectively, to inhibit root growth (Ma et al., 2014; Yin et al., 2015; Qin et al., 2017). Studies in *Arabidopsis* show that auxin mainly functions on epidermal, ABA on cortical, and GA on endodermal cells to control root growth (Vaseva et al., 2018). Taken together, we propose a modulatory model by which ethylene coordinates different hormone signals to control/inhibit specific root growth processes (Figure 9). At the early stages of primary root growth in loose soil, ethylene is maintained at low levels, inducing minimal activation of *OsYUC8*, *OsGA2ox1*, *OsGA2ox2*, *OsGA2ox3*, *OsGA2ox5*, *MHZ4/ABA4*, and *MHZ5/CRTISO* by

OsEIL1. With high levels of bioactive GAs and basal levels of endogenous auxin and ABA, primary root growth is uninhibited and proceeds rapidly. As root growth continues downward, soil impedance and oxygen-deficiency activate ethylene production (Potocka and Szymanowska-Pulka, 2018), and soil compaction restricts diffusion of ethylene (Pandey et al., 2021), leading to higher levels of OsEIL1 in the roots. Activation of auxin and ABA biosynthesis, and GA catabolism, by OsEIL1 ultimately results in the cessation of primary root growth. Our results reveal a novel mechanism underlying primary root development in young rice seedlings. As this mechanism is linked with potentially desirable plant height phenotypes, this study provides molecular avenues for targeted breeding of rice cultivars with optimized root architectures for different soil profiles and properties.

Materials and methods

Plant materials and growth conditions

Rice (*O. sativa* ssp. *japonica*) varieties were grown in a field at the Experimental Station of the Chinese Academy of Agricultural Sciences in Beijing during the natural growing season. Field-grown plants were transferred to pots for photographing. Knockout mutants *slr1*, *ein2*, and *eil1*; overexpressing mutants *OsEIN2* (*EIN2-OX*) and *OsEIL1* (*EIL1-OX*); and myc-tagged *OsEIL1-myc* transgenic lines in a Nip background were described previously (Ma et al., 2013; Li et al., 2015; Yang et al., 2015; Qin et al., 2017).

Soil experiments were performed as previous described (Pandey et al., 2021). Briefly, rice seeds were germinated in the dark for 2 days at 28°C in Petri dishes containing moist filter paper. Germinated seeds were transferred onto the top of packed soil in a glass cylinder and covered with a 1 cm layer of loose top soil. Seedlings were grown for 12 days in a growth chamber under a 14-h light (30°C)/10-h dark (25°C) photoperiod, with a light intensity of ~150 μmol m^{-2} s^{-1} (white light) and 60% relative humidity. Root development was observed at various time points by flushing the soil with tap water and root length was analyzed using ImageJ software.

Generation of *OsGA2ox3* transgenic rice plants

Nip and Zhonghua 11 (ZH11) were the wild-type lines used for transformation. To generate OX (*OsGA2ox3-OX*) plants, the full coding sequence of *OsGA2ox3* was cloned into the plant expression vector pCAMBIA1307 under control of the *CaMV 35S* promoter. Knockout (*osga2ox3*) mutants were created via CRISPR/Cas9-mediated gene editing in the Nip, *EIL1-OX*, and *eil1* backgrounds. The *OsGA2ox3pro:GUS* construct was generated by cloning the 2,600-bp region upstream of the *OsGA2ox3* start codon into pCAMBIA1381Z. OX constructs were introduced into ZH11, while the GUS reporter was introduced into Nip by *Agrobacterium*-mediated transformation. The *OsGA2ox3-OX eil1* plants were generated by crossing *OsGA2ox3-OX* plants with the *eil1* mutant line. About 110 F2 plants were identified by genotyping PCR. We further identified the *OsGA2ox3-OX eil1* in transcript levels and two independent lines were used for further analysis. The phenotype of all F1 and F2 hybrids was the same as those of the parental cultivars. Primers used for plasmid construction are listed in Supplemental Table S1.

Chemical treatment of rice seedlings

GA_3 (Solarbio, G8040) and paclobutrazol (PAC, Solarbio, P8790) were dissolved in ethanol. Germinated rice seeds (~30 seeds) were placed on cheesecloth on a stainless steel sieve, which was placed in an air-tight 10-L plastic box and incubated at 28°C. Seeds were treated with 6 L of water containing various concentrations of GA_3 (0, 1, 10, or 50 μM) or PAC (0, 0.1, 1, or 10 μM).

Ethylene treatment was performed as previously described (Yang et al., 2015). For phenotypic analyses, root length was analyzed using Image J software. For expression analysis, 4-day-old seedlings were treated with 10 μL/L ethylene for the indicated lengths of time at 28°C.

X-ray CT imaging

X-ray CT imaging was performed as previous described (Pandey et al., 2021). Briefly, the root systems of 4-day-old rice seedlings were imaged non-destructively in the soil mesocosms using a GE Phoenix v|tome|x M 240 kV X-ray tomography system (GE Inspection Technologies, Wunstorf, Germany) at the Hounsfield Facility, University of Nottingham. Scans were acquired by collecting 2520 projection images at 140 kV, 200 μA, and 131 ms exposure time in FAST mode (5-min total scan time) at 45 μm scan resolution. Three-dimensional image reconstruction was performed using Datos|REC software (GE Inspection Technologies, Wunstorf, Germany). As root length was the key measurement for the study, a polyline tool in VGStudioMAX V2.2 (Volume graphics GmbH, Germany) was used to segment the roots from the soil.

Quantitative real-time PCR

Total RNA extracted from root tissues are different stages of development using an Ultrapure RNA Kit (CWBIO, CW0581M) according to manufacturer's instructions. Approximately 2 μg total RNA was reverse transcribed to cDNA with HiScript II Q RT SuperMix (Vazyme, R223-01) according to manufacturer's instructions. qPCR was performed as previously described (Zhang et al., 2012), using rice *Actin1* as an internal standard to normalize gene expression. The qPCR primers are listed in Supplemental Table S1.

β-Glucuronidase staining

For GUS staining, roots were collected from 4-day-old *OsGA2ox3p:GUS* transgenic plants, incubated on ice in 90% (v/v) acetone solution for 0.5 h, washed three times with GUS staining buffer (50 mM sodium phosphate, pH 7.0; 10 mM EDTA; 0.5 mM $K_3[Fe(CN)_6]$; 0.5 mM $K_4[Fe(CN)_6]$; 0.1% [v/v] Triton X-100), and incubated in GUS staining buffer containing 1 mM 5-bromo-4-chloro-3-indolyl-β-D-

glucuronic acid for 12 h at 37°C. Samples were rinsed with 70% (v/v) ethanol until the tissue cleared for photography.

LUC transient expression assay

Transient dual LUC expression assays were performed using rice protoplasts and tobacco (*Nicotiana tabacum*) leaves. The reporter plasmid (*OsGA2ox3pro:LUC*) and the effector plasmid (*35S:OsEIL1*), or empty vector controls, were transformed into *Agrobacterium tumefaciens* strain GV3101. Cells were resuspended in infiltration buffer (10 mM MES, 0.2 mM acetosyringone, and 10 mM $MgCl_2$) to a final optical density OD_{600} = 1. Equal amounts of different vectors were infiltrated into the young leaves of 5-week-old tobacco plants using a needleless syringe. After growing the plants in the dark for 12 h, infiltrated plants were cultivated under a 16-h light/8-h dark cycle for 48 h at 24°C. Before observation, leaves were sprayed with 100 mM luciferin (Promega, E1602) and placed in the dark for 5 min. A low-light cooled CCD imaging apparatus (iXon; Andor Technology) was used to observe the LUC activity of each sample.

To quantitatively analyze normalized LUC (LUC/REN) activity, rice protoplasts were prepared and transfected with the corresponding constructs via polyethylene glycol-mediated transfected as previously described (Bart et al., 2006). Firefly LUC and Renilla LUC (REN) activities were measured with a dual-LUC reporting assay kit (Promega, E1980). LUC activity was normalized to REN activity and the relative LUC/REN ratios were calculated. For each plasmid combination, five independent transformations were performed.

ChIP-PCR assay

The ChIP-PCR assay was performed as previously described (Saleh et al., 2008). Approximately 2 g of root tissue from Nip and *OsEIL1-myc* transgenic plants was cross-linked in 1% (v/v) formaldehyde under a vacuum. Chromatin was extracted from the samples and fragmented via ultrasound treatment to a size of 200–500 bp and 3% of the yield was set aside as input template. The OsEIL1–DNA complex was coimmunoprecipitated with anti-myc antibody (Abmart, 324572, 1:3,000 dilution) and protein A/G beads (Invitrogen) or with protein A/G beads alone for the no-antibody control. The precipitated DNA was analyzed by PCR and qPCR using primers listed in Supplemental Table S1.

Electrophoretic mobility shift assay

Plasmid construction and purification of GST-tagged N-terminal OsEIL1 protein domain (amino acids 1–350) were performed as previously described (Qin et al., 2017). Single-stranded complementary oligonucleotide fragments containing putative EIL1-binding elements from the *OsGA2ox3* promoter, or deliberately mutated binding sites, were synthesized and biotinylated (Sangon Biotech). Biotin end-labeled and unlabeled oligonucleotide pairs were annealed to obtain double-stranded biotin-labeled and unlabeled probes by mixing equal amounts of each single-stranded complementary oligonucleotide fragment, incubating the fragments at 95°C for 5 min, and cooling them to room temperature slowly overnight. Probe sequences are given in Supplemental Table S1.

EMSA was performed using a LightShift Chemiluminescent EMSA Kit (Thermo Fisher, 20148) according to manufacturer's instructions. Reaction solutions were incubated for 20 min at room temperature. The protein–probe mixture was separated on a 5% native polyacrylamide gel and transferred to a nylon membrane (GE). Following crosslinking under UV light, DNA on the membrane was detected using a Chemiluminescent Nucleic Acid Detection Module (Thermo Fisher, 89880), according to the manufacturer's instructions.

Vibratome and confocal imaging

Rice tissue sections were generated as previously described (Truernit et al., 2008). Root apices (~5 mm) of 4-days-old seedlings were fixed in 50% (v/v) methanol, 10% (v/v) glacial acetic acid at 4°C for at least 12 h, rinsed with distilled water, and incubated in 1% (v/v) periodic acid at room temperature for 40 min. Root tissue was again rinsed with water and incubated in Schiff reagent with propidium iodide (100 mM sodium metabisulfite and 0.15 N HCl; propidium iodide freshly added to a final concentration of 100 mg/mL) for 1–2 h or until plants were visibly stained.

To obtain cross-sectional images, the root segments were embedded in 3% (w/v) agar and transverse sections (40 μm) were cut with a vibratome (Leica VT 1000 S). Samples were transferred onto microscope slides and covered with a chloral hydrate solution (4 g chloral hydrate, 1 mL glycerol, and 2 mL water), and subsequently imaged with a ZEISS LSM980 confocal microscope using the UV laser. Root meristem size and cell number were determined as described previously (Li et al., 2015). Briefly, root meristem size was defined by measuring the length from the quiescent center to the first elongated epidermal cell. Cell number in the root meristem was determined by counting cortical cells from the quiescent center to the first expanding cortical cells in the fourth cortical layer of the root meristem.

Quantification of endogenous GA levels

To measure GA levels, roots at different stages of development were harvested and used to detect GA_1, GA_3, GA_4, GA_8, GA_{29}, GA_{34}, and GA_{51} levels as previously described (Jiang et al., 2016), using $[^2H_2]$ GA_1 (1.00 ng/g), $[^2H_2]$ GA_3 (1.00 ng/g), $[^2H_2]$ GA_4 (1.00 ng/g), $[^2H_2]$ GA_8 (2.00 ng/g), $[^2H_2]$ GA_{29} (2.00 ng/g), $[^2H_2]GA_{34}$ (2.00 ng/g), and $[^2H_2]$ GA_{51} (2.00 ng/g) as internal standards. Briefly, roots were weighed and ground to fine powder in liquid nitrogen. Internal standards were added to the samples followed by extraction with 10 mL acetonitrile at 4°C for 12 h. The supernatants were sequentially passed through preconditioned tandem solid-phase extraction cartridges containing C18 adsorbent (50 mg) and strong anion exchange adsorbent (200 mg). The strong anion exchange cartridge was then rinsed with 2 mL of 20% methanol (v/v) and GAs were eluted by 3 mL acetonitrile with 1% formic acid (v/v).

The eluent was evaporated under a mild liquid nitrogen stream at 35°C and re-dissolved in 400 μL methanol. Liquid chromatography–tandem mass spectrometry analysis was performed on a UPLC system (Waters) coupled with the 6500 Q-Trap system (AB SCIEX) (Xin et al., 2020). GA measurements were performed by Greensword Creation Technology Company. Each series of experiments was performed in biological triplicates.

Ethylene measurement

Ethylene emission was measured as described previously (Qin et al., 2019), with minor modifications. Twenty seedlings per sample were transferred to a container with 1/2× Murashige & Skoog medium. After culturing under a 14-h light/10-h dark cycle at 28°C for 24 h, 1 mL of gas was collected from each container and used to measure ethylene concentrations with a gas chromatograph (Hitachi, Tokyo, Japan).

Statistical analysis

Student's *t* test was used for significant difference analysis between two samples. One-way ANOVA followed with Tukey's test ($P < 0.05$) was used for pairwise multiple comparisons. All the analyses were performed with GraphPad Prism 5 software. Data for all statistical analyses are shown in Supplemental Data Set S1.

Accession numbers

Sequence data from this article can be found in the GenBank database under the following accession numbers: *OsActin1*, LOC_Os03g50885; *OsGA2ox1*, LOC_Os05g06670; *OsGA2ox2*, LOC_Os01g22910; *OsGA2ox3*, LOC_Os01g55240; *OsGA2ox4*, LOC_Os05g43880; *OsGA2ox5*, LOC_Os07g01340; *OsGA2ox6*, LOC_Os04g44150; *OsGA2ox7*, LOC_Os01g11150; *OsGA2ox8*, LOC_Os05g48700; *OsGA2ox9*, LOC_Os02g41954; *OsGA2ox10*, LOC_Os05g11810; *OsEIL1*, LOC_Os03g20790; *ERF73*, LOC_Os09g11460; *ERF63*, LOC_Os09g11480; *ERF2*, LOC_Os06g08340; *IAA20*, LOC_Os06g07040; and *SHR5*, LOC_Os08g10310.

Supplemental data

Supplemental Figure S1. Ethylene inhibits cell proliferation in the root meristem and promotes radial expansion of cortical cells in the root elongation zone.

Supplemental Figure S2. SLR1-mediated GA signaling is partially required for ethylene-inhibited primary root growth.

Supplemental Figure S3. OsEIL1 activates the promoter activity of *OsGA2ox3* in a transient expression assay in tobacco leaves.

Supplemental Figure S4. OsEIL1 binds to the *OsGA2ox* promoters to activate their expression.

Supplemental Figure S5. Agronomic traits of *OsGA2ox3* knockout and OX mutant lines.

Supplemental Figure S6. Transgenic lines overexpressing *OsGA2ox3* show inhibition of cell proliferation in the root meristem.

Supplemental Figure S7. OsGA2ox3 functions downstream of OsEIL1 to regulate cell proliferation in the root meristem.

Supplemental Table S1. Primers used in this study.

Supplemental Data Set S1. Data for all statistical analyses performed in this study.

Acknowledgments

We thank J.-S. Zhang from the Institute of Genetics and Developmental Biology, Chinese Academy of Sciences for sharing the *ein2*, *EIN2-OX*, *eil1*, and *EIL1-OX* seeds. We also thank Yu Zhao from the Huazhong Agricultural University for sharing the *slr1* seeds. Finally, we thank B. Cai (Greensword Creation Technology Co.) for GA measurements.

Funding

This work was funded by the National Key R&D Program of China grant 2020YFE0202300 to R.Q.; the National Natural Science Foundation of China grants 32030079, 31801445, 31871551, and 32101651 to R.H., G.H., and H.Q.; and the Agricultural Science and Technology Innovation Program of Chinese Academy of Agricultural Sciences.

Conflict of interest statement. The authors declare no conflict of interest.

References

Achard P, Vriezen WH, Van Der Straeten D, Harberd NP (2003) Ethylene regulates *Arabidopsis* development via the modulation of DELLA protein growth repressor function. Plant Cell **15**: 2816–2825

An F, Zhang X, Zhu Z, Ji Y, He W, Jiang Z, Li M, Guo H (2012) Coordinated regulation of apical hook development by gibberellins and ethylene in etiolated *Arabidopsis* seedlings. Cell Res **22**: 915–927

Bart R, Chern M, Park CJ, Bartley L, Ronald PC (2006) A novel system for gene silencing using siRNAs in rice leaf and stem-derived protoplasts. Plant Methods **2**: 13

Correa J, Postma JA, Watt M, Wojciechowski T (2019) Soil compaction and the architectural plasticity of root systems. J Exp Bot **70**: 6019–6034

de Dorlodot S, Forster B, Pages L, Price A, Tuberosa R, Draye X (2007) Root system architecture: Opportunities and constraints for genetic improvement of crops. Trends Plant Sci **12**: 474–481

Fukao T, Bailey-Serres J (2008). Ethylene—a key regulator of submergence responses in rice. Plant Sci **175**: 43–51

Hattori Y, Nagai K, Furukawa S, Song XJ, Kawano R, Sakakibara H, Wu J, Matsumoto T, Yoshimura A, Kitano H, et al. (2009) The ethylene response factors SNORKEL1 and SNORKEL2 allow rice to adapt to deep water. Nature **460**: 1026–1030

Ikeda A, Ueguchi-Tanaka M, Sonoda Y, Kitano H, Koshioka M, Futsuhara Y, Matsuoka M, Yamaguchi J (2001) Slender rice, a constitutive gibberellin response mutant, is caused by a null mutation of the SLR1 gene, an ortholog of the height-regulating gene GAI/RGA/RHT/D8. Plant Cell **13**: 999–1010

Jiang Z, Xu G, Jing Y, Tang W, Lin R (2016) Phytochrome B and REVEILLE1/2-mediated signalling controls seed dormancy and germination in *Arabidopsis*. Nat Commun **7**: 12377

Kuroha T, Nagai K, Gamuyao R, Wang DR, Furuta T, Nakamori M, Kitaoka T, Adachi K, Minami A, Mori Y, et al. (2018) Ethylene–gibberellin signaling underlies adaptation of rice to periodic flooding. Science **361**: 181–186

Lee HY, Yoon GM (2018) Regulation of ethylene biosynthesis by phytohormones in etiolated rice (*Oryza sativa* L.) seedlings. Mol Cells **41**: 311–319

Li H, Torres-Garcia J, Latrasse D, Benhamed M, Schilderink S, Zhou W, Kulikova O, Hirt H, Bisseling T (2017) Plant-specific histone deacetylases HDT1/2 regulate GIBBERELLIN 2-OXIDASE2 expression to control *Arabidopsis* root meristem cell number. Plant Cell **29**: 2183–2196

Li JT, Zhao Y, Chu HW, Wang LK, Fu YR, Liu P, Upadhyaya N, Chen CL, Mou TM, Feng YQ, et al. (2015) SHOEBOX modulates root meristem size in rice through dose-dependent effects of gibberellins on cell elongation and proliferation. PLoS Genet **11**: e1005464

Lo SF, Yang SY, Chen KT, Hsing YI, Zeevaart JA, Chen LJ, Yu SM (2008) A novel class of gibberellin 2-oxidases control semidwarfism, tillering, and root development in rice. Plant Cell **20**: 2603–2618

Ma B, Yin CC, He SJ, Lu X, Zhang WK, Lu TG, Chen SY, Zhang JS (2014) Ethylene-induced inhibition of root growth requires abscisic acid function in rice (*Oryza sativa* L.) seedlings. PLoS Genet **10**: e1004701

Ma B, He SJ, Duan KX, Yin CC, Chen H, Yang C, Xiong Q, Song QX, Lu X, Chen HW, et al. (2013) Identification of rice ethylene-response mutants and characterization of MHZ7/OsEIN2 in distinct ethylene response and yield trait regulation. Mol Plant **6**: 1830–1848

Marcon C, Paschold A, Hochholdinger F (2013) Genetic control of root organogenesis in cereals. Methods Mol Biol **959**: 69–81

Okamoto T, Takahashi T (2019) Ethylene signaling plays a pivotal role in mechanical-stress-induced root-growth cessation in *Arabidopsis thaliana*. Plant Signal Behav **14**: 1669417

Pandey BK, Huang GQ, Bhosale R, Hartman S, Sturrock CJ, Jose L, Martin OC, Karady M, Voesenek LACJ, Ljung K, et al. (2021) Plant roots sense soil compaction through restricted ethylene diffusion. Science **371**: 276–280

Potocka I, Szymanowska-Pulka J (2018) Morphological responses of plant roots to mechanical stress. Ann Bot **122**: 711–723

Qin H, He L, Huang R (2019) The coordination of ethylene and other hormones in primary root development. Front Plant Sci **10**: 874

Qin H, Zhang Z, Wang J, Chen X, Wei P, Huang R (2017) The activation of OsEIL1 on YUC8 transcription and auxin biosynthesis is required for ethylene-inhibited root elongation in rice early seedling development. PLoS Genet **13**: e1006955

Qin H, Wang J, Chen X, Wang F, Peng P, Zhou Y, Miao Y, Zhang Y, Gao Y, Qi Y, et al. (2019) Rice OsDOF15 contributes to ethylene-inhibited primary root elongation under salt stress. New Phytol **223**: 798–813

Rogers ED, Benfey PN (2015) Regulation of plant root system architecture: implications for crop advancement. Curr Opin Biotechnol **32**: 93–98

Sakai M, Sakamoto T, Saito T, Matsuoka M, Tanaka H, Kobayashi M (2003) Expression of novel rice gibberellin 2-oxidase gene is under homeostatic regulation by biologically active gibberellins. J Plant Res **116**: 161–164

Saleh A, Alvarez-Venegas R, Avramova Z (2008) An efficient chromatin immunoprecipitation (ChIP) protocol for studying histone modifications in *Arabidopsis* plants. Nat Protoc **3**: 1018–1025

Shekhar V, Stckle D, Thellmann M, Vermeer JEM (2019) The role of plant root systems in evolutionary adaptation. Curr Top Dev Biol **131**: 55–80

Street IH, Aman S, Zubo Y, Ramzan A, Wang X, Shakeel SN, Kieber JJ, Schaller GE (2015) Ethylene inhibits cell proliferation of the *Arabidopsis* root meristem. Plant Physiol **169**: 338–350

Taylor I, Lehner K, McCaskey E, Nirmal N, Ozkan-Aydin Y, Murray-Cooper M, Jain R, Hawkes EW, Ronald PC, Goldman DI, et al. (2021) Mechanism and function of root circumnutation. Proc Natl Acad Sci USA **118**: e2018940118

Tian HY, Jia YB, Niu TT, Yu QQ, Ding ZJ (2014) The key players of the primary root growth and development also function in lateral roots in *Arabidopsis*. Plant Cell Rep **33**: 745–753

Truernit E, Bauby H, Dubreucq B, Grandjean O, Runions J, Barthelemy J, Palauqui JC (2008) High-resolution whole-mount imaging of three-dimensional tissue organization and gene expression enables the study of Phloem development and structure in *Arabidopsis*. Plant Cell **20**: 1494–1503

Ubeda-Tomas S, Federici F, Casimiro I, Beemster GT, Bhalerao R, Swarup R, Doerner P, Haseloff J, Bennett MJ (2009) Gibberellin signaling in the endodermis controls *Arabidopsis* root meristem size. Curr Biol **19**: 1194–1199

Vaseva II Qudeimat E, Potuschak T, Du Y, Genschik P, Vandenbussche F, Van Der Straeten D (2018) The plant hormone ethylene restricts *Arabidopsis* growth via the epidermis. Proc Natl Acad Sci USA **115**: E4130–E4139

Verma V, Ravindran P, Kumar PP (2016) Plant hormone-mediated regulation of stress responses. BMC Plant Biol **16**: 86

Wang SJ, Ho CH, Chen HW (2011) Rice develop wavy seminal roots in response to light stimulus. Plant Cell Rep **30**: 1747–1758

Xin PY, Guo QH, Li BB, Cheng SJ, Yan JJ, Chu JF (2020) A tailored high-efficiency sample pretreatment method for simultaneous quantification of 10 classes of known endogenous phytohormones. Plant Commun **1**: 100047

Yamada M, Han XW, Benfey PN (2020) RGF1 controls root meristem size through ROS signalling. Nature **577**: 85–88

Yamauchi T, Tanaka A, Mori H, Takamure I, Kato K, Nakazono M (2016) Ethylene-dependent Aerenchyma formation in adventitious roots is regulated differently in rice and maize. Plant Cell Environ **39**: 2145–2157

Yamauchi T, Yoshioka M, Fukazawa A, Mori H, Nishizawa NK, Tsutsumi N, Yoshioka H, Nakazono M (2017) An NADPH oxidase RBOH functions in rice roots during lysigenous aerenchyma formation under oxygen-deficient conditions. Plant Cell **29**: 775–790

Yang C, Ma B, He SJ, Xiong Q, Duan KX, Yin CC, Chen H, Lu X, Chen SY, Zhang JS (2015) MAOHUZI6/ETHYLENE INSENSITIVE3-LIKE1 and ETHYLENE INSENSITIVE3-LIKE2 regulate ethylene response of roots and coleoptiles and negatively affect salt tolerance in rice. Plant Physiol **169**: 148–165

Yin CC, Ma B, Collinge DP, Pogson BJ, He SJ, Xiong Q, Duan KX, Chen H, Yang C, Lu X, et al. (2015) Ethylene responses in rice roots and coleoptiles are differentially regulated by a carotenoid isomerase-mediated abscisic acid pathway. Plant Cell **27**: 1061–1081

Yoon J, Cho LH, Yang W, Pasriga R, Wu Y, Hong WJ, Bureau C, Wi SJ, Zhang T, Wang R, et al. (2020) Homeobox transcription factor OsZHD2 promotes root meristem activity in rice by inducing ethylene biosynthesis. J Exp Bot **71**: 5348–5364

Yukiyoshi K, Karahara I (2014) Role of ethylene signalling in the formation of constitutive aerenchyma in primary roots of rice. AoB Plants **6**: plu043

Zhang ZJ, Wang J, Zhang RX, Huang RF (2012) The ethylene response factor AtERF98 enhances tolerance to salt through the transcriptional activation of ascorbic acid synthesis in *Arabidopsis*. Plant J **71**: 273–287

Zheng H, Pan X, Deng Y, Wu H, Liu P, Li X (2016) AtOPR3 specifically inhibits primary root growth in *Arabidopsis* under phosphate deficiency. Sci Rep **6**: 24778